reaction between $PQ^{\bullet+}$ and PS-$(PTZ)_4(PTZ^{\bullet+})$ (Table II) where electrostatic repulsion is considerably less. The importance of electrostatic effects is also suggested by qualitative observations which show that the recombination rate for the polymer bound species can increase dramatically with increasing ionic strength.

In the three-polymer system, the reduced acceptor, PS-$PQ^{\bullet+}$, is stable under the conditions of the experiment. However, when no added donor PTZ is present in the solution, 9-$MeAn^{\bullet+}$ undergoes an irreversible reduction that removes it from the system. Addition of PTZ at high enough concentrations to intercept 9-$MeAn^{\bullet+}$ before it decomposes leads to a considerably enhanced stability.

Acknowledgment. This research was supported by grants from the National Science Foundation (Grant no. CHE-8503092) and the Army Research Office, Durham. J.O. acknowledges California State University for a sabbatical leave and the University of North Carolina for a visiting appointment for the time period which this work was performed.

Registry No. 9-Me-An, 779-02-2.

Electronic Structure of Low-Spin Ferric Porphyrins: A Single-Crystal EPR and Structural Investigation of the Influence of Axial Ligand Orientation and the Effects of Pseudo-Jahn–Teller Distortion

Robert Quinn, Joan Selverstone Valentine,* Marianne P. Byrn, and Charles E. Strouse*

Contribution from the Department of Chemistry and Biochemistry, the J. D. McCullough X-ray Crystallography Laboratory, and the Solid State Science Center, University of California, Los Angeles, California 90024. *Received September 19, 1986*

Abstract: X-ray structure determinations are reported for the (tetraphenylporphyrinato)iron(III) complexes of the substituted imidazole ligands *cis*- and *trans*-methylurocanate (cMU and tMU, respectively). Both complexes are six-coordinate and low-spin. The cMU ligand has an internal hydrogen bond, while the tMU ligand is hydrogen bonded to a THF solvate molecule. Crystals of the cMU complex contain two crystallographically independent centrosymmetric cations; these species differ in the orientation of the imidazole ligands with respect to the porphyrin. Single-crystal EPR **g**-tensor determinations for the two forms of the cMU complex reveal that the ligand orientation influences both the distribution of spin density in the complex and the energies of the highest occupied molecular orbitals. This influence appears to arise in part from the direct interaction between metal and axial ligand π orbitals and in part through pseudo-Jahn–Teller induced distortion of the porphyrin ligand. Crystal data: $FeTPP(cMU)_2SbF_6 \cdot 1.5$toluene, space group $P\bar{1}$, $Z = 2$, $a = 10.406$ (5) Å, $b = 11.752$ (4) Å, $c = 28.538$ (10) Å, $\alpha = 103.34$ (3)°, $\beta = 108.35$ (3)°, $\gamma = 106.18$ (3)° at 115 K; $FeTPP(tMU)_2SbF_6 \cdot 2THF$, space group $P\bar{1}$, $Z = 1$, $a = 9.898$ (3) Å, $b = 12.600$ (4) Å, $c = 15.344$ (8) Å, $\alpha = 99.99$ (3)°, $\beta = 112.82$ (3)°, $\gamma = 114.58$ (2) at 115 K.

The common occurrence of histidine as an axial ligand in heme proteins has prompted the synthesis of numerous analogues designed to explore the role of this ligand in heme chemistry. Several aspects of the imidazole–heme interaction have attracted attention. Substitution and hydrogen bonding induced changes in ligand basicity have been explored spectroscopically and electrochemically.[1,2] EPR characterization of the electronic structure has been particularly useful in this regard. X-ray structural investigations have indicated that changes in the orientation of the axial ligands with respect to the porphyrin affect the Fe–N bond lengths and the thermodynamic stability.[3] It appears that in some situations this effect is sufficient to alter the spin state of the complex.[4] The influence of the relative orientations of two axial ligands on the spectroscopic and electrochemical properties has also been discussed.[5] The structural investigations reported herein were initiated to characterize the hydrogen bonding in two isomeric iron(III)–imidazole complexes. The occurrence of two conformers in the crystal structure of one of these complexes has been exploited through single-crystal **g**-tensor determination. This determination has provided a detailed picture of the ways in which the orientation of the axial ligands with respect to the porphyrin ligand influences the electronic structure.

The observation that the histidyl imidazole ligands of hemoproteins are usually hydrogen bonded to another group on the protein[6] has led to the hypothesis that such hydrogen bonding might alter the chemical properties of the heme moiety.[1] Coordination of imidazolate, the limit of strongly hydrogen bonded imidazole, leads to ferric porphyrin complexes with properties quite different from those of the analogous imidazole complexes.[7,8] Differences in the IR and electrochemical properties of a series of complexes of the form $FeTPP(L)_2SbF_6$[9] where L is imidazole or a substituted imidazole have demonstrated that the mode of hydrogen bonding to coordinated imidazole has a substantial effect on these properties.[1] Included in this series were two new imidazole complexes in which the isomeric ligands, *cis*-methylurocanate

(1) Quinn, R.; Mercer-Smith, J.; Burstyn, J. N.; Valentine, J. S. *J. Am. Chem. Soc.* **1984**, *106*, 4136–4144.
(2) Walker, F. A.; Reis, D.; Balke, V. L. *J. Am. Chem. Soc.* **1984**, *106*, 6888–6898.
(3) Scheidt, W. R.; Chipman, D. M. *J. Am. Chem. Soc.* **1986**, *108*, 1163–1167.
(4) Geiger, D. K.; Lee, Y. J.; Scheidt, W. R. *J. Am. Chem. Soc.* **1984**, *106*, 6339–6343.
(5) Walker, F. A.; Huynh, B. H.; Scheidt, W. R.; Osvath, S. R. *J. Am. Chem. Soc.* **1986**, *108*, 5288–5297.
(6) Valentine, J. S.; Sheridan, R. P.; Allen, L. C.; Kahn, P. C. *Proc. Natl. Acad. Sci. U.S.A.* **1979**, *76*, 1009–1013.
(7) Quinn, R.; Nappa, M.; Valentine, J. S. *J. Am. Chem. Soc.* **1982**, *104*, 2588–2595.
(8) Quinn, R.; Strouse, C. E.; Valentine, J. S. *Inorg. Chem.* **1983**, *22*, 3934–3940.
(9) Abbreviations used are as follows: TPP, tetraphenylporphinato; tMU, *trans*-methylurocanate; cMU *cis*-methylurocanate; ImH, imidazole; 2MeImH, 2-methylimidazole; 1MeIm, 1-methylimidazole; P, porphyrin; L, ligand; EPR, electron paramagnetic resonance; THF, tetrahydrofuran; OAc, acetate; OEP, octaethylporphinato.

0002-7863/87/1509-3301$01.50/0

(cMU) and *trans*-methylurocanate (tMU), differ in their mode of hydrogen bonding. IR studies have shown that the tMU ligand can hydrogen bond in an intermolecular fashion to various acceptor molecules. By contrast, the configuration of the cMU ligand is such that the N–H moiety is permanently hydrogen bonded to an ester carbonyl oxygen atom. The cMU isomer thus serves as a model for hydrogen bonding of the coordinated histidyl of heme proteins to peptide backbone carbonyls. Structural investigations of these complexes were undertaken to confirm the differing modes of hydrogen bonding as deduced spectroscopically and to evaluate the effects of such hydrogen bonding on the Fe–N(ligand) bond lengths.

Single-crystal EPR characterization[10] of a series of $Fe^{III}TPP$ complexes with axial sulfur donors has demonstrated the relationship between ligand orientation and spin distribution in low-spin ferric porphyrin complexes. Such measurements also provide crystal field parameters particularly sensitive to the axial ligand binding. When the structural determination for the cMU compound revealed the presence of two crystallographically independent complexes with differing ligand orientations, a single-crystal EPR investigation of this material was undertaken to provide a spectroscopic assessment of the effect of ligand orientation on the electronic structure and to confirm the predicted relationship between ligand orientation and spin distribution.

Experimental Section

Solvent purification, ligand synthesis and purification, and the synthesis and recrystallization of $FeTPP(cMU)_2SbF_6$ and $FeTPP(tMU)_2SbF_6$ have been described previously.[1]

Crystal Growth. Crystals of $FeTPP(cMU)_2SbF_6$ for X-ray diffraction analysis were grown by layering 10 mL of a 4 mM solution of $FeTPP(cMU)_2SbF_6$ in CH_2Cl_2 with toluene. After 2 weeks at room temperature, large, well-formed crystals were separated by filtration. The X-ray analysis indicated the presence of 1.5 toluene molecules of solvation per formula unit. Anal. Calcd $C_{137}H_{112}N_{16}O_8Fe_2Sb_2F_{12}$: C, 61.09; H, 4.19; N, 8.32. Found: C, 60.41; H, 4.33; N, 8.15.

Crystals of $FeTPP(tMU)_2SbF_6$ suitable for X-ray analysis could not be obtained by recrystallization from CH_2Cl_2/toluene. The crystals obtained were brittle and diffracted very poorly. Elemental analysis results for this material were consistent with one toluene of solvation per formula unit. Anal. Calcd for $C_{65}H_{52}N_8O_4FeSbF_6$: C, 60.02; H, 4.03; N, 8.62. Found: C, 58.06; H, 4.01; N, 8.52.

The use of the solvent system CH_2Cl_2/THF produced crystals suitable for X-ray characterization. A 3.0-mL portion of THF was layered on top of 2.0 mL of 2.5 mM $FeTPP(tMU)_2SbF_6$ in CH_2Cl_2. After 2 weeks at room temperature, the solvent was removed by filtration and a crystal chosen for X-ray analysis.

Data Collection and Structure Determinations. Mounting and data collection methods for both crystals were essentially the same. The crystals were coated with epoxy, mounted on a Syntex $P\bar{1}$ diffractometer, and cooled to −158 °C. Three standard reflections were measured every 97 reflections during the data collection. No significant changes were observed. A summary of the conditions of data collection, crystal parameters, and agreement factors can be found in Table I. All data analysis made use of the UCLA Crystallographic Computing Package. Scattering factors and anomalous dispersion corrections were taken from ref 11.

$FeTPP(tMU)_2SbF_6$ crystallized as a triclinic crystal with two molecules of THF per formula unit, $Z = 1$, space group $P\bar{1}$. Because the 0,0,1 reflection was measured inaccurately, it was removed from the data set. Direct methods (MULTAN) led to the location of the iron (0.5,0.5,0.5) and antimony (1.0,1.0,1.0) atoms at crystallographic inversion centers and to the location of all non-hydrogen atoms. Following several cycles of full-matrix least-squares refinement, many of the hydrogen atoms, including the one bonded to the noncoordinated nitrogen atom of the ligand, were located in a difference map. Positions of all hydrogen atoms were then calculated with idealized bond lengths and angles and held constant during subsequent refinements. The thermal parameters of two phenyl carbon atoms, C_{18} and C_{19}, were unusually large with respect to those of other carbon atoms of the same ring, possibly as a result of interaction with the THF molecule of solvation. Refinement of the positional and anisotropic thermal parameters of all non-hydrogen atoms led to final agreement factors of $R = 0.044$ and $R_w = 0.51$, supporting the choice of $P\bar{1}$ as the space group.

Table I. Summary of Data Collection and Crystal Parameters

compd	$FeTPP(cis)_2SbF_6 \cdot 1.5C_7H_8$	$FeTPP(trans)_2SbF_6 \cdot 2THF$
temp, °C	−158	−158
crystal dim., mm	0.15, 0.15, 0.20	0.20, 0.25, 0.25
space group	$P\bar{1}$	$P\bar{1}$
Z	2	1
unit cell		
a, Å	10.406 (5)	9.898 (3)
b, Å	11.752 (4)	12.600 (4)
c, Å	28.538 (10)	15.344 (8)
α, deg	103.34 (3)	99.99 (3)
β, deg	108.35 (3)	112.82 (3)
γ, deg	106.18 (3)	114.58 (2)
radiation	Mo Kα (λ = 0.71069 Å)	Mo Kα (λ = 0.71069 Å)
scan method	θ–2θ	θ–2θ
scan range, $2\theta_{max}$, deg	50	50
scan rate, deg min^{-1}	8.0	6.0
criterion for obsd	$I_o > 3\sigma(I_o)$	$I_o > 3\sigma(I_o)$
unique obsd data	5216	3783
R	7.1	4.4
R_w	7.7	5.1
error of fit	2.00	1.41
data-to-parameter ratio	10.1	9.5

$Fe^{III}TPP(cMU)_2SbF_6$ crystallized as a triclinic crystal with 1.5 toluene molecules of solvation per formula unit, $Z = 2$, and space group $P\bar{1}$. The structure was solved by direct methods (MULTAN). The two iron atoms are located at crystallographic inversion centers, (1.0,1.0,1.0) and (1.0,1.0,0.5). The two resulting centrosymmetric $FeTPP(cMU)_2^+$ complexes are designated A and B. Difference Fourier maps and least-squares refinement led to the location of all non-hydrogen atoms. Both toluene molecules of solvation were modeled as rigid groups. The positions and orientations of the groups along with the diagonal and off-diagonal elements of a group thermal motion tensor were refined.[12] One toluene molecule was disordered about an inversion center; it was modeled as a rigid group with 50% occupancy. The other toluene molecule was also disordered and was modeled as two rigid groups, each initially at 50% occupancy. Refinement of the occupancy parameter gave a 45:55 occupancy ratio for the two groups. Refinement of the positions and anisotropic thermal parameters of the SbF_6^- and subsequent difference maps indicated that it was also disordered. The anion was modeled as two rigid groups. The diagonal and off-diagonal components of the translation, libration, and screw motion tensors were refined along with an occupancy factor (the S tensor was constrained to be traceless).[12] Refinement led to a final Sb–Sb distance of 0.622 Å and an occupancy ratio of 47:53.

Following refinement of atomic positions and thermal parameters, Fourier synthesis resulted in the location of many hydrogen atoms. Those of the toluene methyl groups and the pyrrole nitrogen atoms of the ligands were not located. The positions of all hydrogen atoms, excluding those of the toluene methyl groups, were calculated on the basis of a C–H distance of 1.00 Å, and these positions were fixed in subsequent refinements. Refinement of atomic positions and the anisotropic thermal parameters of all axial ligand atoms, porphyrin nitrogen atoms, and iron atoms resulted in final agreement factors of $R = 0.071$ and $R_w = 0.077$.

Single-Crystal EPR Measurements. Equipment and methods used in the **g**-tensor determination were similar to those reported previously.[10,13] A fitting procedure was used to refine the zero-point in the rotation about each axis,[14] and the analysis was modified to allow accurate extraction of g values for the case where the three rotation axes are coplanar. All EPR measurements were made at 77 K; X-ray alignments were carried out at 115 K. In all, g values were measured as a function of rotation about six different axes. Principal **g** values and corresponding crystal field parameters were extracted from ten different combinations of three rotations. In each combination the minimum angle between any pair of rotation axes was 40°. The multiple determinations provide an experimental measure of the uncertainty in the derived parameters (see Table II). Assignment of the two EPR signals to the two crystallographically

(10) Byrn, M. P.; Katz, B. A.; Keder, N. L.; Levan, K. R.; Magurany, C. J.; Miller, K. M.; Pritt, J. W.; Strouse, C. E. *J. Am. Chem. Soc.* **1983**, *105*, 4916–4922.

(11) *International Tables of X-ray Crystallography*; Kynoch Press: Birmingham, England, 1974.

(12) Schomaker, J.; Trueblood, K. N. *Acta Crystallogr.* **1968**, *B24*, 63–76.

(13) Byrn, M. P.; Strouse, C. E. *J. Magn. Reson.* **1983**, *53*, 32–39.

(14) The zero positions were refined by minimizing the sum of the differences of the duplicate determinations of the three diagonal elements of the **g** tenor.[13]

Table II. Single-Crystal EPR Parameters

	molecule A	molecule B
g_1	1.481 (18)	1.486 (11)
g_2	2.265 (9)	2.298 (10)
g_3	2.999 (10)	2.965 (13)
Δ^a	3.22 (9)	3.02 (8)
V^a	1.77 (3)	1.84 (3)
V/Δ^a	0.551 (14)	0.609 (18)
g_1/Z^b	89.6 (3)	86.3 (3)
g_2/X^b	27.7 (10)	11.2 (6)
g_3/Z^b	3.0 (6)	5.9 (5)

[a] Crystal field parameters, in units of the spin–orbit coupling constant, were derived by the method of Taylor.[25] [b] Angles between the principal axes of the g tensor and the molecular axes. Z is the porphyrin normal and X is the Fe–N(1) vector.

Table III. Unit Cell Atomic Coordinates of $FeTPP(trans)_2SbF_6 \cdot 2THF$

atom	x	y	z
Fe	0.5000 (0)	1.5000 (0)	0.5000 (0)
N(1)	0.6330 (5)	1.4150 (4)	0.5183 (3)
N(2)	0.4677 (5)	1.4785 (4)	0.3601 (3)
C(1)	0.6999 (6)	1.3857 (4)	0.6015 (3)
C(2)	0.7787 (6)	1.3184 (5)	0.5830 (4)
C(3)	0.7601 (7)	1.3059 (5)	0.4893 (4)
C(4)	0.6701 (6)	1.3669 (4)	0.4487 (4)
C(5)	0.6203 (6)	1.3685 (4)	0.3516 (3)
C(6)	0.5262 (6)	1.4225 (4)	0.3109 (3)
C(7)	0.4784 (7)	1.4288 (5)	0.2114 (4)
C(8)	0.3889 (7)	1.4867 (5)	0.1997 (4)
C(9)	0.3837 (6)	1.5198 (4)	0.2921 (3)
C(10)	0.3064 (6)	1.5841 (4)	0.3093 (3)
C(11)	0.6694 (7)	1.3074 (5)	0.2861 (4)
C(12)	0.8414 (7)	1.3620 (5)	0.3122 (4)
C(13)	0.8866 (7)	1.3039 (6)	0.2516 (4)
C(14)	0.7589 (8)	1.1915 (6)	0.1655 (4)
C(15)	0.5876 (8)	1.1359 (6)	0.1402 (4)
C(16)	0.5427 (7)	1.1931 (5)	0.2001 (4)
C(17)	0.2201 (7)	1.6215 (5)	0.2265 (4)
C(18)	0.0484 (10)	1.5478 (7)	0.1584 (6)
C(19)	0.0322 (10)	1.5844 (8)	0.0839 (8)
C(20)	0.0597 (8)	1.6939 (6)	0.0758 (4)
C(21)	0.2320 (8)	1.7676 (6)	0.1438 (5)
C(22)	0.3134 (7)	1.7308 (6)	0.2181 (5)
N(3)	0.7164 (5)	1.6677 (4)	0.5600 (3)
N(4)	0.9331 (5)	1.8648 (4)	0.6623 (3)
C(23)	0.7930 (7)	1.7649 (5)	0.6493 (4)
C(24)	0.9497 (6)	1.8327 (5)	0.5776 (4)
C(25)	0.8146 (6)	1.7094 (4)	0.5156 (4)
C(26)	1.0865 (7)	1.9190 (5)	0.5670 (4)
C(27)	1.0935 (7)	1.8964 (5)	0.4812 (4)
C(28)	1.2380 (8)	1.9882 (6)	0.4751 (5)
C(29)	1.3516 (9)	2.0252 (6)	0.3653 (6)
O(1)	1.3609 (6)	2.0877 (4)	0.5431 (4)
O(2)	1.2145 (5)	1.9450 (4)	0.3805 (3)
Sb	1.0000 (0)	1.0000 (0)	1.0000 (0)
F(1)	0.9093 (4)	0.9546 (3)	0.8575 (2)
F(2)	0.8342 (4)	0.8364 (3)	0.9736 (2)
F(3)	1.1541 (4)	0.9480 (3)	1.0066 (2)
C(30)	0.6422 (9)	0.8588 (7)	0.1159 (5)
C(31)	0.5262 (11)	0.7165 (7)	0.0594 (5)
C(32)	0.6529 (11)	0.6744 (6)	0.0858 (5)
C(33)	0.7953 (13)	0.7700 (7)	0.1922 (6)
O(3)	0.7950 (6)	0.8843 (4)	0.2033 (3)

[a] Numbers in parentheses following atomic coordinates are estimated standard deviations.

independent complex ions was made on the basis of the angle between the largest principal axes of the g tensor and the normals to the two porphyrin ligands.

Results and Discussion

Structure of $Fe^{III}TPP(tMU)_2SbF_6 \cdot 2THF$. The unit cell of this compound contains one porphyrin complex cation, one SbF_6 anion, and two THF molecules of solvation. Both the Fe and Sb atoms are located at crystallographic inversion centers. The THF molecules are hydrogen bonded to NH groups of the axial ligands.

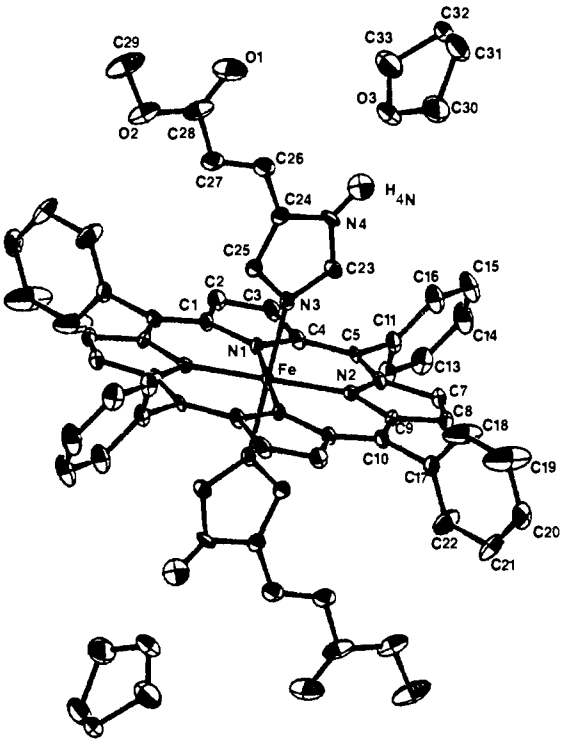

Figure 1. ORTEP plot of $FeTPP(tMU)_2SbF_6$. Hydrogen atoms except H(N4) have been omitted for clarity.

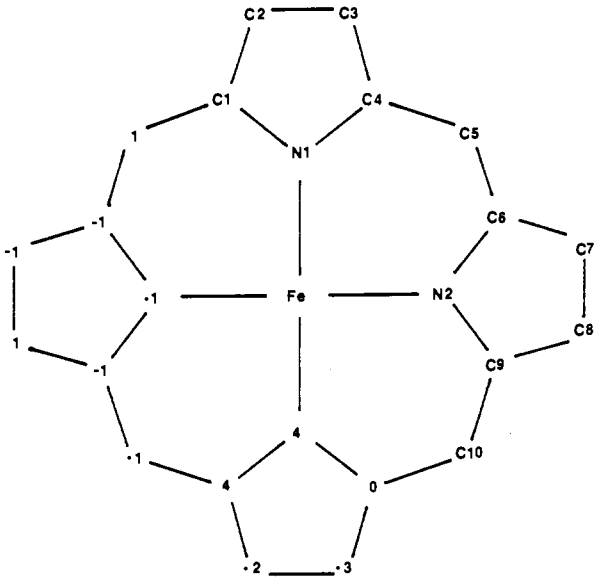

Figure 2. Displacements in units of 0.01 Å from the mean plane of the 24 atom porphyrin core of $FeTPP(tMU)_2SbF_6$.

The structure of the $FeTPP(tMU)_2^+$ complex and the numbering scheme are illustrated in Figure 1. Atomic coordinates are listed in Table III. Perpendicular displacements in units of 0.01 Å from the least-squares plane of the 24 core atoms are illustrated in Figure 2. Compared to other TPP complexes, these deviations are quite small.[6]

Bond lengths and angles for the porphyrin core, the axial ligand, the anion, and the solvate molecule are listed in Tables IV and V. The Fe–N(porphyrin bond lengths of 1.988 (4) and 1.995 (4) Å are consistent with those of other low-spin ferric porphyrin complexes.[15] The average value of 1.992 (5) Å is insignificantly different from that of 1.989 (8) Å found[16] for $FeTPP(ImH)_2Cl$. The Fe–N(ligand) bond length is 1.983 (4) Å and the N(lig-

(15) Scheidt, W. R.; Reed, C. A. *Chem. Rev.* **1981**, *81*, 543–555.
(16) Collins, D. M.; Countryman, R.; Hoard, J. L. *J. Am. Chem. Soc.* **1972**, *94*, 2066–2072.

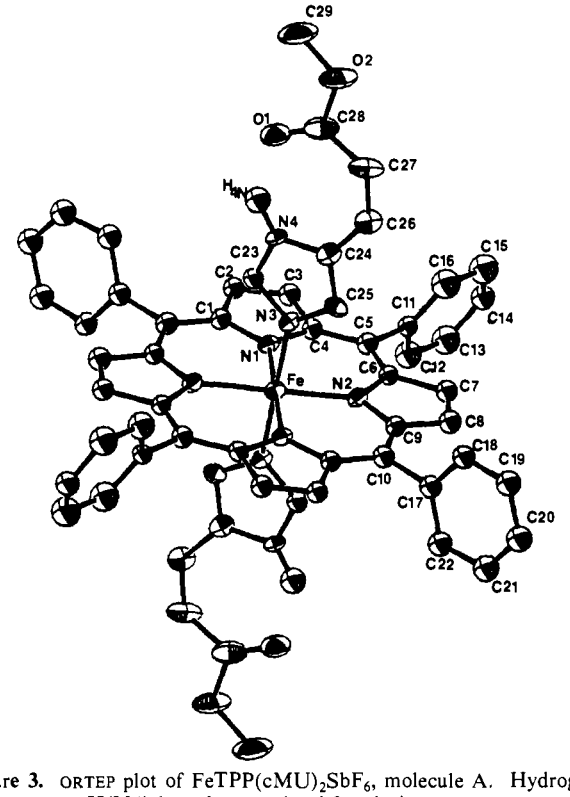

Figure 3. ORTEP plot of $FeTPP(cMU)_2SbF_6$, molecule A. Hydrogen atoms except H(N4) have been omitted for clarity.

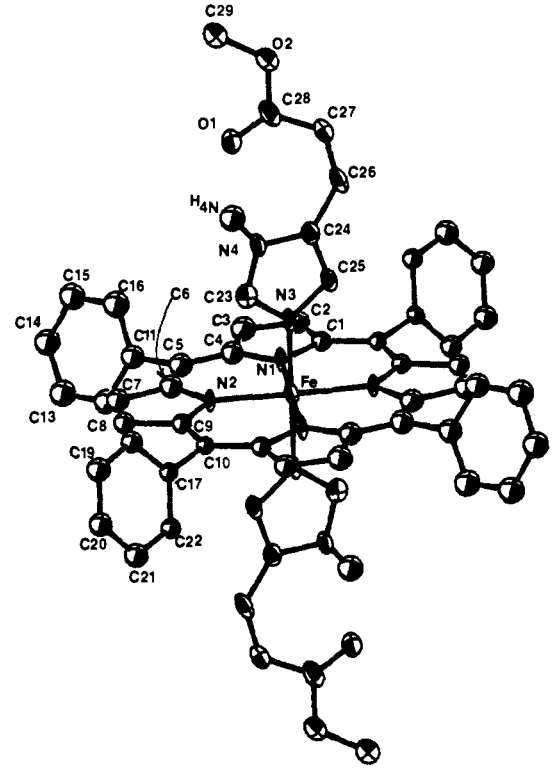

Figure 4. ORTEP plot of $FeTPP(cMU)_2SbF_6$, molecule B. Hydrogen atoms except H(N4) have been omitted for clarity.

and)–Fe–N(porphyrin) bond angles are 90.3 (2) and 89.7 (2)°. The dihedral angle between the plane of the imidazole ring and the porphyrin plane is 86°. The angle between the imidazole plane and the Fe–N(2) vector is 22°. There are short nonbonding distances between the ligand hydrogen atoms H(23) and H(25) and the porphyrin nitrogen and carbon atoms. These interactions are summarized in Table VI.

The five-membered imidazole ring of the ligand is essentially planar with the five ring atoms displaced less than 0.007 Å from the least-squares plane. The methylacrylate substituent is also planar, excluding the methyl carbon atom. Displacements from the least-squares plane defined by C(26), C(27), C(28), O(1), and O(2) are 0.008 Å or less. The plane of the methylacrylate is tilted by 10° with respect to the plane of the imidazole ring. A dihedral angle of similar magnitude has been reported for *trans*-urocanic acid dihydrate where the plane of the carboxylate is tilted by 7.3° with respect to the plane of the imidazole ring.[17]

The Sb–F bond lengths are 1.879 (3), 1.868 (3), and 1.871 (3) Å. The average value of 1.873 (6) Å is longer than the value of 1.844 (5) Å reported[18] for $KSbF_6$. The F–Sb–F bond angles are 89.4 (2), 90.1 (2), and 90.6 (2)°. The anion is located near the ligand N–H bond with a F(1)–N(4) distance of 3.15 Å and a N–H–F angle of 112°. Since the F–N distance is greater than the sum of the van der Waals radii[19] of F and N, any hydrogen bonding interaction between the anion and the axial ligand is very weak.

Structure of $Fe^{III}TPP(cMU)_2SbF_6 \cdot 1.5C_7H_8$. The structure of the independent centrosymmetric molecules of $FeTPP(cMU)_2^+$, designated A and B, are illustrated in Figures 3 and 4. The numbering scheme used is analogous to that of the tMU complex. Atomic coordinates are listed in Table VII. Perpendicular displacements from the least-squares plane of 24 core atoms are illustrated in Figure 5. These displacements are remarkably small as are those of the tMU complex.

Bond lengths and angles for the porphyrin core and axial ligand atoms are collected in Tables VII and IX. The Fe–N(p) bond lengths are 1.996 (7) and 1.998 (7) Å in molecule A and 1.983 (7) and 2.007 (6) Å in molecule B. The average Fe–N(p) distance for the four independent measurements is 1.996 (10) Å, in substantial agreement with that of $Fe^{III}TPP(tMU)_2SbF_6$, 1.992 (5) Å, and other low-spin ferric porphyrin complexes.[15] The Fe–N(ligand) bond lengths are 1.967 (7) and 1.979 (7) Å for molecules A and B, respectively. The N(porphyrin)–Fe–N(ligand) bond angles are 90.5 (3) and 89.8 (3)° for molecule A and 90.8 (3) and 89.5 (3)° for molecule B. The orientation of the ligands with respect to a N(p)–Fe–N(p) axis is not equivalent for the two independent molecules. The angle ϕ, defined as the angle between the N–Fe–N axis and the projection of the ligand normal onto the porphyrin plane, is 29° for molecule A and 15° for molecule B. As summarized in Table VI, the nonbonding interaction distances of molecule B ligand hydrogen atoms are slightly shorter than those for molecule A or for the tMU complex.

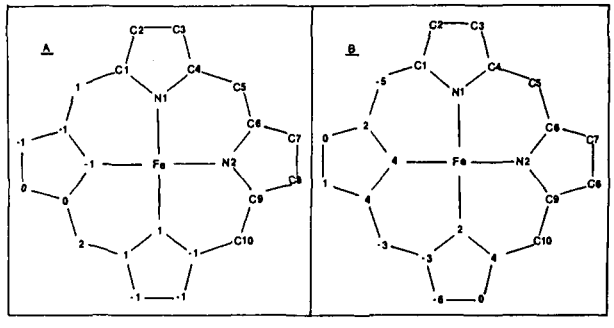

Figure 5. Displacements in units of 0.01 Å from the mean plane of the 24 atom porphyrin core of $FeTPP(cMU)_2SbF_6$.

The aromatic imidazole rings of both molecules are essentially planar, with the five ring atoms displaced 0.005 Å or less from the mean plane. The methylacrylate substituents (excluding the methyl carbon atom) of both ligands are significantly less planar than that of the tMU ligand. Displacements as large as 0.08 Å from the five-atom mean acrylate plane are observed for the cMU ligands. Similar to the tMU ligand, the mean plane of the methylacrylate is tilted by 10° with respect to the imidazole ring for molecule A and 16° for molecule B.

(17) Hawkinson, S. W. *Acta Crystallogr.* **1977**, *B33*, 2288–2291.
(18) Kruger, G. J.; Pistorius, C. W. F. T.; Heyns, A. M. *Acta Crystallogr.* **1976**, *B32*, 2916–2918.

Table VII. Coordinates in the Unit Cell[a]

atom	*x*	*y*	*z*	atom	*x*	*y*	*z*
	$FeTPP(cis)_2SbF_6$, Molecule A				$FeTPP(cis)_2SbF_6$, Molecule B		
Fe(A)	1.0000 (0)	1.0000 (0)	1.0000 (0)	Fe(B)	1.0000 (0)	1.0000 (0)	0.5000 (0)
N(1A)	0.8868 (7)	1.1106 (6)	1.0058 (3)	N(1B)	1.0947 (7)	0.9238 (6)	0.4583 (3)
N(2A)	1.0266 (7)	1.0438 (6)	0.9392 (3)	N(2B)	0.8761 (7)	0.8273 (6)	0.4934 (3)
C(1A)	0.8225 (9)	1.1301 (8)	1.0411 (3)	C(1B)	1.2048 (9)	0.9855 (8)	0.4454 (3)
C(2A)	0.7484 (9)	1.2158 (8)	1.0314 (3)	C(2B)	1.2400 (10)	0.8971 (8)	0.4133 (3)
C(3A)	0.7685 (10)	1.2452 (8)	0.9908 (3)	C(3B)	1.1512 (10)	0.7794 (9)	0.4060 (4)
C(4A)	0.8541 (9)	1.1808 (8)	0.9740 (3)	C(4B)	1.0611 (10)	0.7961 (8)	0.4348 (4)
C(5A)	0.8965 (10)	1.1887 (8)	0.9332 (3)	C(5B)	0.9596 (10)	0.6964 (8)	0.4378 (4)
C(6A)	0.9755 (9)	1.1243 (8)	0.9170 (3)	C(6B)	0.8773 (10)	0.7138 (8)	0.4668 (4)
C(7A)	1.0190 (9)	1.1318 (8)	0.8739 (3)	C(7B)	0.7670 (10)	0.6108 (8)	0.4697 (4)
C(8A)	1.0938 (10)	1.0570 (8)	0.8707 (4)	C(8B)	0.7035 (9)	0.6615 (8)	0.4974 (3)
C(9A)	1.1006 (9)	1.0030 (8)	0.9108 (3)	C(9B)	0.7708 (9)	0.7973 (8)	0.5127 (3)
C(10A)	1.1735 (10)	0.9215 (8)	0.9197 (3)	C(10B)	0.7298 (9)	0.8838 (7)	0.5406 (3)
C(11A)	0.8597 (9)	1.2798 (8)	0.9062 (3)	C(11B)	0.9333 (10)	0.5631 (8)	0.4067 (4)
C(12A)	0.7489 (12)	1.2340 (10)	0.8560 (4)	C(12B)	0.8036 (10)	0.4914 (9)	0.3626 (4)
C(13A)	0.7179 (12)	1.3194 (10)	0.8308 (4)	C(13B)	0.7815 (11)	0.3691 (9)	0.3327 (4)
C(14A)	0.7977 (10)	1.4466 (9)	0.8559 (4)	C(14B)	0.8878 (11)	0.3217 (9)	0.3468 (4)
C(15A)	0.9065 (12)	1.4888 (10)	0.9041 (4)	C(15B)	1.0164 (11)	0.3894 (9)	0.3910 (4)
C(16A)	0.9393 (11)	1.4060 (9)	0.9296 (4)	C(16B)	1.0397 (11)	0.5133 (9)	0.4217 (4)
C(17A)	1.2498 (10)	0.8883 (8)	0.8853 (4)	C(17B)	0.6046 (9)	0.8324 (7)	0.5554 (3)
C(18A)	1.1704 (10)	0.7927 (8)	0.8366 (4)	C(18B)	0.6160 (9)	0.7730 (8)	0.5925 (3)
C(19A)	1.2401 (11)	0.7634 (9)	0.8042 (4)	C(19B)	0.4928 (10)	0.7268 (8)	0.6042 (4)
C(20A)	1.3877 (11)	0.8312 (9)	0.8196 (4)	C(20B)	0.3665 (10)	0.7399 (8)	0.5796 (4)
C(21A)	1.4656 (11)	0.9255 (9)	0.8675 (4)	C(21B)	0.3529 (10)	0.7987 (8)	0.5422 (4)
C(22A)	1.4014 (10)	0.9560 (9)	0.9023 (4)	C(22B)	0.4749 (9)	0.8458 (8)	0.5302 (3)
N(3A)	0.8175 (7)	0.8567 (6)	0.9506 (3)	N(3B)	0.8454 (7)	0.9873 (6)	0.4349 (3)
N(4A)	0.5912 (7)	0.7164 (7)	0.9190 (3)	N(4B)	0.7261 (8)	1.0323 (6)	0.3676 (3)
C(23A)	0.7016 (10)	0.8097 (9)	0.9614 (4)	C(23B)	0.8553 (10)	1.0631 (8)	0.4066 (4)
C(24A)	0.6367 (10)	0.7010 (8)	0.8783 (4)	C(24B)	0.6239 (10)	0.9312 (8)	0.3702 (4)
C(25A)	0.7782 (10)	0.7882 (8)	0.8987 (3)	C(25B)	0.6999 (10)	0.9041 (7)	0.4119 (4)
C(26A)	0.5522 (10)	0.6132 (8)	0.8248 (4)	C(26B)	0.4668 (10)	0.8710 (8)	0.3381 (4)
C(27A)	0.4097 (11)	0.5320 (9)	0.8005 (4)	C(27B)	0.3761 (10)	0.8980 (8)	0.3018 (4)
C(28A)	0.3017 (12)	0.5146 (10)	0.8240 (5)	C(28B)	0.4117 (11)	1.0015 (9)	0.2816 (4)
C(29A)	0.0491 (12)	0.4132 (12)	0.8022 (5)	C(29B)	0.3064 (11)	1.1129 (9)	0.2317 (4)
O(1A)	0.3186 (7)	0.5577 (6)	0.8695 (3)	O(1B)	0.5336 (7)	1.0733 (5)	0.2894 (3)
O(2A)	0.1696 (8)	0.4373 (7)	0.7855 (3)	O(2B)	0.2885 (7)	1.0106 (6)	0.2529 (3)

[a] Numbers in parentheses following atomic coordinates are estimated standard deviations.

The averaged bond lengths of $Fe^{III}TPP(cMU)_2SbF_6$ and $Fe^{III}TPP(tMU)_2SbF_6$ are compared to those of $FeTPP(ImH)_2Cl$[16] in Table X. Agreement among the three is within experimental error for each chemically distinct bond length.

Hydrogen Bonding to Coordinated Ligands. Both the cMU and tMU ligands are involved in hydrogen bonding interactions. In the tMU complex the N(4)–O(3) distance of 2.801 (5) Å is shorter than the sum of the van der Waals radii[19] of oxygen and nitrogen, 3.07 Å, and implies a hydrogen bonding interaction. Further, the N(4)–O(3) distance is somewhat shorter than the average N–O hydrogen bonding distance[20] of 2.93 ± 0.11 Å.

The structural data are consistent with an intramolecular hydrogen bond in the cMU ligand. The N(4)–O(1) distances observed for molecules A and B are 2.614 (11) 2.727 (11) Å, respectively. Hydrogen bonding to carbonyls generally occurs at an H–O–C angle of 120°.[21] In the present structure H–O–C angles of 120 and 121° are observed for molecules A and B, respectively.

The structures of other metalloporphyrin complexes in which imidazole ligands are hydrogen bonded have been reported. In $Co^{III}TPP(ImH)_2OAc$, the acetate counterion is hydrogen bonded to imidazole ligands of adjacent molecules with N–O interaction distances of 2.74 (2) and 2.69 (2) Å.[22] The chloride counterion of $FeTPP(ImH)_2Cl{\cdot}CH_3OH$ is hydrogen bonded to imidazole with a N–Cl distance of 3.07 Å, while the other imidazole ligand is weakly hydrogen bonded to CH_3OH at a N–O distance of 2.90 Å.[16] Hydrogen bonding interactions[23] occur between ClO_4^- and ImH ligands in $FeOEP(ImH)_2ClO_4$, but interaction distances were not reported.

Table XI. Fe–N(L) Bond Lengths and ϕ of Ferric Porphyrin Imidazole Complexes

complex	Fe–N(L) bond length, Å	ϕ, deg	N(p)···H(L), Å	ref
$FeTPP(ImH)_2Cl$	1.957 (4)	39	2.79	16
	1.991 (5)	18	2.56–2.58	
$Fe^{III}PPIX(NMeIm)_2$	1.966 (5)	16	2.51, 2.60	b
	1.988 (5)	3	2.51, 2.54	
$FeOEP(ImH)_2ClO_4$	2.01	7	*a*	24
$FeTPP(ImH)_2Cl$	1.977	6	*a*	5
	1.964	41		
$FeTPP(trans)_2SbF_6$	1.983 (4)	22	2.61, 2.62	tw
$FeTPP(cis)_2SbF_6$				
molecule A	1.967 (7)	29	2.61, 2.72	tw
molecule B	1.979 (7)	15	2.53, 2.56	

[a] Not reported. [b] Little, R. G.; Dymock, K. R.; Ibers, J. A. *J. Am. Chem. Soc.* **1975**, *97*, 4532–4539.

Comparison of the Iron–Ligand Bond Lengths. The Fe–N(ligand) bond lengths of $Fe^{III}TPP(tMU)_2SbF_6$, $Fe^{III}TPP(cMU)_2SbF_6$, and other imidazole complexes of ferric porphyrins are compared in Table XI. In addition to hydrogen bonding effects, the $pK_a(BH^+)$ of the ligand and the orientation of the ligand with respect to a N(p)–Fe–N(p) axis may influence axial bond lengths. Maximum steric interactions between ligand hydrogen atoms and porphyrin nitrogen atoms occur at $\phi = 0$. As

(19) Bondi, A. J. *J. Phys. Chem.* **1964**, *68*, 441–451.
(20) Vinogradov, S. N.; Linnell, R. H. *Hydrogen Bonding*; Van Nostrand: Reinhold, New York 1971.
(21) Donohue, J. In *Structural Chemistry and Molecular Biology*; Rich, A., Davidson, N., Eds.; W. H. Freeman Co.: San Francisco, 1968; p 443–456.
(22) Little, R. G.; Dymock, K. R.; Ibers, J. A. *J. Am. Chem. Soc.* **1975**, *97*, 4532–4539.
(23) Kirner, J. F.; Hoard, J. L. *Abstracts of Papers*, 175th National Meeting of the American Chemical Society; American Chemical Society: Washington, DC, 1978; Inorg. 14.

summarized in Table XI, it has generally been observed that for porphyrin complexes with imidazole ligands having different orientations, the ligand with the larger ϕ, and thus with longer nonbonding interaction distances, exhibits the shorter axial bond length. For $Fe^{III}TPP(cMU)_2SbF_6$, angles of ϕ = 29 and 15 for molecules A and B, respectively, lead to the expectation of inequivalent axial bond lengths, with molecule A having the shorter length. This is indeed observed, but the difference in the experimental values of 1.967 (7) Å for molecule A and 1.979 (7) Å for molecule B is comparable to the experimental uncertainty. The Fe–N(ligand) bond length of $Fe^{III}TPP(tMU)_2SbF_6$ is 1.983 (4) Å, with the axial ligand oriented at ϕ = 22°. Within the experimental accuracy this bond length is indistinguishable from that of molecule B in the cMU material.

Assessment of the effects of the $pK_a(BH^+)$ of the ligand on the axial bond length is difficult. As the ligand becomes more basic, the Fe–N(ligand) bond length would reasonably be expected to shorten. Structural data for ferric porphyrin complexes of substituted imidazoles of various basicities are quite limited. However, comparison of the ImH,[16] cMU, and tMU ligands oriented at similar values of ϕ (18,15, and 22°, respectively) indicates that the axial bond lengths differ by only 0.012 Å or less for ligands representing a greater than 100-fold range of basicities. The pK_a of tMU, cMU, and ImH are 4.93, 5.58 and 7.11,[1,24] respectively, while the observed axial bond lengths at 1.983 (4), 1.979 (7), and 1.991 (5) Å, respectively.

The effect of hydrogen bonding can be viewed in a context similar to the pK_a effects. That is, hydrogen bonding to coordinated imidazoles can be thought of as partial ligand deprotonation. As the strength of hydrogen bonding is increased, the ligand becomes more basic and a shortening of the Fe–N(ligand) bond length is expected. The limit of strong hydrogen bonding is imidazolate and the decrease in axial bond length resulting from imidazolate coordination can be taken as an upper limit for hydrogen bonding effects. A reasonable value for this upper limit is 0.06 Å, the apparent difference in the axial bond lengths[8,16] of $FeTPP(4MeIm)_2^-$ and $FeTPP(ImH)_2^+$. Since hydrogen bonding interactions to coordinated imidazole will, in reality, likely result in a "degree of deprotonation" substantially less than that of Im^-, the difference in the axial bond length of a non-hydrogen bonded imidazole and a hydrogen bonded imidazole will likely be significantly less than 0.06 Å. Both the cMU and tMU complexes reported here were found to contain hydrogen bonded imidazole ligands with N–H···O distances in the range 2.6–2.8 Å. One would thus expect that any difference in Fe–N_a distance arising from a difference in the nature of the hydrogen bonding would be small compared to the experimental uncertainty.

EPR Measurements. The *g*-value anisotropy observed in low-spin d^5 transition-metal complexes provides a very powerful probe of electronic structure. Analysis of the principal *g*-values, which can be obtained fron. polycrystalline or frozen solution samples, provides a measure of the energies of the two low-lying excited states of the system, from which the relative energies of the three d^π orbitals can be inferred. The orientations of the principal axes of the **g** tensor, available from single-crystal EPR measurements, provide wave functions (i.e., assignments) for these three orbitals. In the case of iron(III) porphyrin complexes, both the energies and wave functions of these orbitals are governed primarily by the nature and orientation of the axial ligands. EPR measurements are thus very sensitive to changes in axial ligation.

The left side of Figure 6 depicts the orbital energy level diagram for a centrosymmetric bis-imidazole complex with the axial ligands eclipsing the Fe–N_p bonds in the *x* direction. The right side of the figure depicts the ground state and the two low-lying excited states of the system labeled in terms of a hole model. The energy level differences in this system are dominated by ligand to metal π donation. In this regard the d_{xy} orbital is "nonbonding", the d_{xz} orbital is higher in energy by virtue of its interaction with the two pyrrole groups in the *x* direction, and the d_{yz} orbital is highest in energy because it interacts with the two pyrrole groups in the

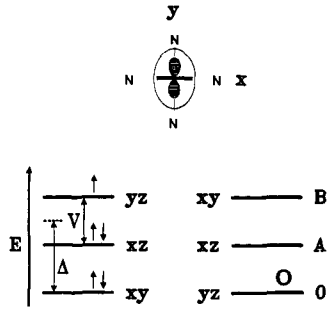

Figure 6. Energy level diagrams for a low-spin $Fe^{III}TPP$ complex with imidazole ligands eclipsing the Fe–N_p bonds.

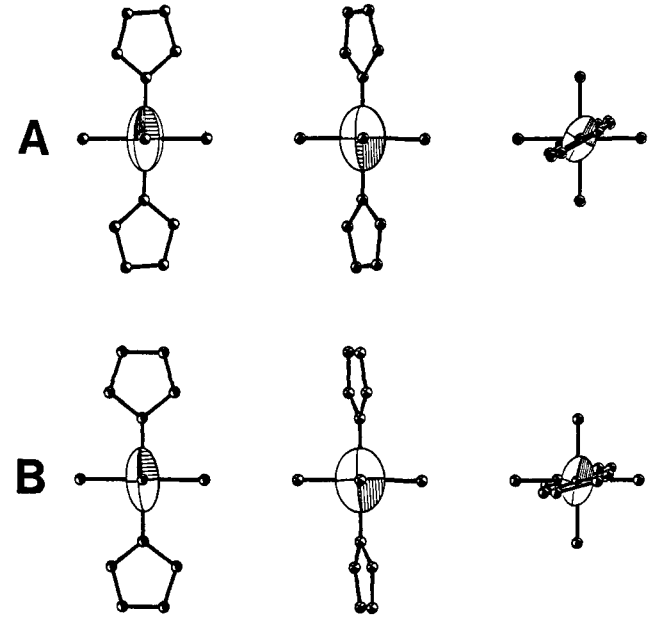

Figure 7. Graphical depictions of the **g** tensors in $FeTPP(cMU)_2$. For each molecule the first view is in the Fe–N(1) direction, the second view is in the Fe–N(2) direction, and the third view is down the porphyrin normal.

y direction as well as the two axial ligands. To the extent that the pyrrole and imidazole ligands do not differ greatly in donor strength, the three levels should be approximately equally spaced, and the ratio of the crystal field parameters V/Δ should be ca. 2/3. Experimental determinations of V/Δ for a wide range of complexes confirm this.[10]

It should be noted here that the energy difference between the d_{xz} and d_{yz} orbitals is dominated by interactions with the axial ligands but that it is also affected by distortions of the porphyrin which can arise from pseudo-Jahn–Teller effects, nonbonding interactions with the axial ligand, porphyrin substitution, and "packing effects" in the crystalline lattice. It will be argued below that in these complexes pseudo-Jahn–Teller effects have an observable effect on the spin density distribution and also give rise to an unexpected dependence of *V* on the axial ligand orientation.

While an exact solution based on the combined crystal field and spin–orbit spin Hamiltonian[25] can be used to relate the crystal field parameters and the EPR observations, a simple perturbation treatment provides more physical insight into the source of the *g*-value anisotropy. Spin–orbit mixing of the first excited state, *xz*, with the ground state *yz*, results in a non-zero L_z and a g_z that exceeds the free electron value, g_0, by $2\lambda/A$.[26] Similarly mixing *xy* into the ground state gives $g_y = g_0 + 2\lambda/B$. Because this

(24) Sundberg, R. J.; Martin R. B. *Chem. Rev.* **1974**, *74*, 471–517.

(25) Taylor, C. P. S. *Biochim. Biophys. Acta* **1977**, *491*, 137–148.

(26) The free ion value of the spin–orbit coupling constant, λ, for iron is 420 cm^{-1}, but this value can be significantly reduced with increased covalency (see: Palmer, G. In *Iron Porphyrins*, Part II; Lever, A. B. P., Gray, H. B. Eds.; Addison Wesley: Reading, MA, 1983; pp 43–88).

Table XII. EPR Parameters for Five $Fe^{III}TPP$ Bis-Imidazole Complexes[a]

ligand	ϕ	g_1	g_2	g_3	ΔFe–N	Fe–N_a	V/λ	Δ/λ	V/Δ	E_{yz}	E_{xz}	pK_a(BH^+)
ImH	6	1.59	2.32	2.84	0.017	1.977	2.16	3.12	0.69	4.20	2.03	7.11
cis(B)	15	1.49	2.30	2.96	0.024	1.979	1.84	3.02	0.61	3.94	2.10	5.58
tMU	22	1.47	2.27	2.96	0.007	1.983	1.80	3.08	0.58	3.98	2.18	4.93
cis(A)	29	1.48	2.26	3.00	0.002	1.967	1.77	3.22	0.55	4.10	2.34	5.58
ImH	41	1.47	2.2	3.00	0.005	1.964	1.72	3.53	0.49	4.39	2.67	7.11

[a] ΔFe–N is the difference between the two Fe–N_p bond lengths.

perturbation treatment does not include simultaneous mixing of the two excited states with the ground state, it predicts that g_x will have the free electron value.

In the orthorhombic case described above, the plane defined by the two largest principal g values coincides with the plane of the partially filled molecular orbital, d_{yz}. In general, however, this is not true. Figure 7 provides a graphical depiction of the **g** tensors determined for the two cMU conformers and illustrates the simple but nonintuitive relationship between the orientations of the axial ligands and the principal axes of the **g** tensor. As the ligand and the half-filled d orbital rotate about the porphyrin normal through an angle ϕ the **g** tensor rotates about the same axis by an angle $-\phi$. This behavior can be derived from a simple extension of the above perturbation treatment. In a coordinate system fixed with respect to the axial ligands, rotation of the porphyrin ligand results in the mixing of $x^2 - y^2$ and xy. This in turn can be shown to result in the retrograde rotation of the **g** tensor.[10,27]

The experimental observations are in good quantitative accord with this simple model. In molecules A and B the largest principal g value, g_3, occurs with the magnetic field 3.0 (6) and 5.9 (5)° from the respective porphyrin normals. The angle between the g_2 principal axis and y, the Fe–N(1) vector, is 27.7 (10)° for molecule A and 11.2 (6)° for molecule B. These angles correspond to the crystallographic ϕ's of 29 and 15°, respectively. While the crystallographic and EPR angles for molecule A are the same within experimental error, the EPR value for molecule B is significantly less than the crystallographic value. This difference is probably associated with the distortion of the porphyrin ligand in molecule B. In this molecule the Fe–N(1) distance is found to be 0.024 Å shorter than the Fe–N(2) distance. This distortion favors the alignment of the partially filled orbital with the Fe–N(1) direction and should thus result in an angle between the g_2 principal axis and Fe–N(1) that is smaller than the crystallographic ϕ.

ϕ Dependence of the Crystal Field Parameters. A rather complete description of the effect of ligand orientation in the nitrogen-donor complexes can be obtained by combining the structural and single-crystal EPR results for $Fe^{III}TPP(cMU)_2SbF_6$ and the structural and polycrystalline EPR measurements for $Fe^{III}TPP(tMU)_2SbF_6$ with the data recently reported for the bis-imidazole complex of $Fe^{III}TPP$ by Walker, Huynh, Scheidt, and Osvath.[5] As in the present investigation, the material characterized by these investigators was found to contain two crystallographically independent centrosymmetric molecules. The ϕ's for these two molecules are 6 and 41°; when combined with the values of 15 and 29° obtained for the cMU complex and 22° obtained for the tMU complex, these five measurements provide very good coverage of the 0–45° range of ligand orientation. While the experimental assignment of g values to crystallographic sites is not available for the complexes observed by Walker et al., the assignment suggested by these authors is consistent with the observations for the cMU complex. The structural and crystal field parameters for the five complexes are summarized in Table XII.

For both pairs of complexes the axial ligand field splitting, Δ, is larger for the species with the larger ϕ. This observation is consistent with the fact that in these and other nitrogen-donor complexes there is a reduction in the Fe–N_a bond distance with increasing ϕ. This reduction has been attributed to a decrease in nonbonding repulsion between the porphyrin nitrogen atoms and hydrogen atoms of the imidazole ligands.

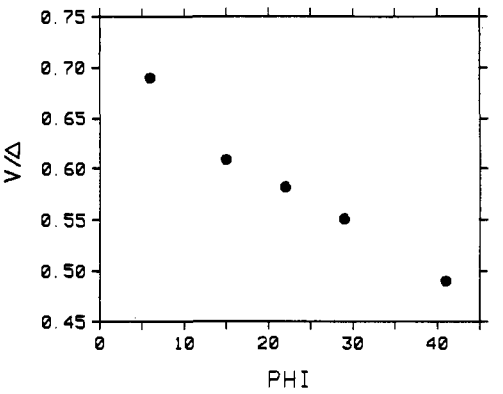

Figure 8. V/Δ vs. ϕ for the five complexes tabulated in Table XII.

On the other hand, for both pairs of complexes the rhombic splitting, V, decreases with increasing ϕ. This trend is counter to the change expected on the basis of the change in axial ligand bond distance. It would appear that some interaction other than that of the d orbitals with the axial ligands is responsible for this change. In d^5 complexes of this type, pseudo-Jahn–Teller distortion of the porphyrin ligand can contribute to the rhombic splitting. A b_{1g} distortion, characterized by shortening of two inversion related Fe–N bonds and lengthening of the other two, is observed in many structure determinations of low-spin $Fe^{III}TPP$ complexes in which the Fe–N_p bonds in (or close to) the plane containing the partially filled d orbital are shorter than those more nearly perpendicular to that plane. The differences in Fe–N_p distances (typically 0.02 Å) are small but sufficient to account for the observed changes in rhombic splitting (vide infra).

The observed structural and spectroscopic differences in the two pairs of conformers (see Table XII) are consistent with the hypothesis that the ϕ dependence of V can be attributed to a pseudo-Jahn–Teller distortion of the porphyrin. In both cases the conformer with low ϕ gives Fe–N_p distances approximately perpendicular to the imidazole plane that are about 0.02 Å shorter than those close to the imidazole plane. (As a measure of the significance of these differences it should be noted that in each pair of conformers the average Fe–N_p distances differ by only 0.002 Å.) One would expect the difference in Fe–N_p distances to decrease to zero as the axial ligand orientation approaches ϕ = 45°. Indeed, the two conformers with high ϕ give indistinguishable Fe–N_p distances. Since changes in axial ligand bond distances on the order of 0.01 Å are associated with changes in Δ on the order of 0.2λ, a change in the difference in the Fe–N_p distances on the order of 0.02 Å is sufficient to account for a change in V on the order of 0.4λ.

The combination of the trends in V and Δ results in the plot of V/Δ vs. ϕ presented in Figure 8. While the lower σ donor strength of the substituted cMU ligand is reflected in smaller values of both V and d than one would expect from interpolation of the values of the unsubstituted species, the two parameters change by approximately the same fraction, and as a result V/Δ is largely independent of the σ donor strength. Similarly, in the previously reported investigation[10] of sulfur donor complexes, V/Δ was found to be largely independent of σ donor strength.

The large variation in rhombicity observed in this series of complexes, V/Δ = 0.49–0.69, must be reconciled with the observations by Walker et al.[2] On the basis of frozen solution

(27) Oosterhuis, W. T.; Lang, G. *Phys. Rev.* **1969**, *178*, 439–456.

measurements for six substituted imidazole complexes of $Fe^{III}TPP$, these investigators found V/Δ to be nearly constant, 0.65 ± 0.02. The results from crystalline and frozen solution samples can be reconciled if it is assumed that in the frozen solutions the complex tends to adopt the low-energy (low ϕ) configuration. A distribution of configurations (with different V/Δ's) could also be masked in the frozen solution measurements since the extraction of g values is likely to be biased toward the extremes which correspond to maximum values of Δ, and in this case minimum values of ϕ.

To the extent that the ϕ dependence of V can be attributed to pseudo-Jahn-Teller distortion of the porphyrin, this ϕ dependence reflects a Jahn-Teller stabilization of the eclipsed ($\phi = 0$) conformation. This is of particular interest because the ϕ dependence of the total energy has been somewhat difficult to rationalize. Nonbonding repulsion between the imidazole hydrogen atoms and the porphyrin nitrogen atoms, to which the ϕ dependence of the $Fe-N_a$ distance is attributed, is a maximum at $\phi = 0$. Yet as documented by Scheidt and Chipman,[3] most imidazole complexes of metalloporphyrins adopt conformations with small ϕ. While there may be other effects, as proposed by Scheidt and Chipman,[3] that contribute to the relative stability of the $\phi = 0$ conformation, the present results indicate that pseudo-Jahn-Teller distortion of the porphyrin ligand cannot be ignored in any computation designed to model the ϕ dependence of the total energy.

Conclusions

EPR observations provide a detailed picture of the changes in electronic structure of ferric porphyrins brought about by changes in axial ligation. In particular, this investigation has demonstrated that rotation of imidazole about the porphyrin normal alters both the spin distribution and the energy of the highest occupied molecular orbital. In heme protein systems a change in the energy of the highest occupied molecular orbital will affect the reduction potential of the ferric species, while a change in spin distribution may alter the pathway and rate of electron transfer into and out of the iron center. By determining the orientations of the axial and porphyrin ligands the protein may thus exert thermodynamic and kinetic control of the electronically "flexible" heme group.

This investigation has also revealed a significant pseudo-Jahn-Teller contribution to the crystal field, the magnitude of which depends on the orientation of the axial ligands. This orientation dependence is observed in the Fe-N distances of the porphyrin ligand, the magnitude of the rhombic splitting, and the distribution of spin density. A mathematical model of the crystal field that includes effects of axial ligand orientation, pseudo-Jahn-Teller distortion, and trans influence in low-spin ferric porphyrin complexes will be described in the next paper in this series.

Acknowledgment. The authors are indebted to the National Institutes of Health (CES GM35329, JSV GM28222) and the National Science Foundation (CES CHE-8340836, JSV CHE-8505473) for financial support, to Dr. Reuel VanAtta for obtaining the polycrystalline EPR spectrum of the tMU complex, and to Prof. Ann Walker and Prof. Robert Scheidt for communication of unpublished results.

Supplementary Material Available: Tables of bond lengths, bond angles, interaction distances, atomic positions, and thermal parameters for all atoms (16 pages); listing of observed and calculated structure factors (40 pages). Ordering information is given on any current masthead page.

Reactions of Iodine with Triphenylphosphine and Triphenylarsine

F. Albert Cotton* and Piotr A. Kibala

Contribution from the Department of Chemistry and Laboratory for Molecular Structure and Bonding, Texas A&M University, College Station, Texas 77843. *Received September 22, 1986*

Abstract: The reaction of PPh_3 with I_2 leads to disproportionation of iodine and formation of $(PPh_3I)^+$ and I_3^-. Dichloroethane solutions of these give $[(PPh_3I)_2I_3]I_3$ (**1**) while toluene solutions give $(PPh_3I)I_3$ (**2**). Both compounds were structurally characterized by X-ray crystallography. The crystallographic data for **1** are as follows: orthorhombic, space group *Pnma* with unit cell dimensions $a = 12.517$ (3) Å, $b = 38.292$ (8) Å, $c = 9.116$ (3) Å, $V = 4369$ (3) Å^3, $Z = 4$. The structure was refined to $R = 0.043$ ($R_w = 0.049$) for 1179 reflections with $I > 3\sigma(I)$. The structure of **1** consists of zigzag chains of $[(PPh_3I)_2I_3]^+$ cations sandwiched in layers of I_3^- anions. The pertinent crystallographic data for **2** are as follows: monoclinic, space group $P2_1/n$ with unit cell dimensions $a = 11.583$ (2) Å, $b = 11.862$ (2) Å, $c = 15.900$ (3) Å, $\beta = 95.44$ (2)°, $V = 2175$ (1) Å^3, $Z = 4$. The structure was refined to $R = 0.042$ ($R_w = 0.051$) for 2264 reflections with $I > 3\sigma(I)$. Molecules of **2** form infinite chains with a distance of 3.741 (1) Å between adjacent ends. The reaction of $AsPh_3$ with I_2 in dichloroethane gives $[(AsPh_3I)_2I_3]I_3$ (**3**), which is isostructural with $[(PPh_3I)_2I_3]I_3$ (**1**).

The discovery of the element iodine, by Bernard Courtois, was reported more than 170 years ago[1a] and the existence[1b] of polyiodides has been known nearly as long. In more recent times it has been recognized that polyiodides exhibit a rich structural chemistry and adopt a variety of geometric arrangements which depend on the cations with which they are associated.[1c] It was well over a hundred years ago that that commenest of all phosphine ligands, triphenylphosphine, was first described by Michaelis and co-workers.[2]

In view of how widely used both of these substances are, and how omnipresent in inorganic research laboratories, it seems truly astonishing that virtually nothing has been reported[3] concerning

(1) (a) Clement, N.; Desormes, C.-B. *Ann. Chim. Phys.* **1813**, *88*, [1], 304. (b) *Gmelins Handbuch der Anorganischen Chemie* [8e Aufluge] **1933**, *8*, 402-431. (c) Tebbe, K.-F. In *Homoatomic Rings, Chains and Macromolecules*; Rheingold, A. L., Ed.; Elsevier: Amsterdam, 1977; Chapter 24.

(2) (a) Michaelis, A.; Gleichman, L. *Ber. Dtsch. Chem. Ges.* **1882**, *15*, 801. (b) Michaelis, A.; Reese, A. *Ibid.* **1882**, *15*, 1610.

0002-7863/87/1509-3308$01.50/0